

## MORPHOLOGY AND PATHOMORPHOLOGY

# Effects of Whole-Body Vibration on Prostate Morphology

V. A. Ananov\*, E. L. Lushnikova, N. A. Abdullaev, A. I. Neymark\*

Translated from *Byulleten' Eksperimental'noi Biologii i Meditsiny*, Vol. 146, No. 11, pp. 573-579, November, 2008  
Original article submitted September 24, 2008

The peculiarities of the prostate remodeling caused by long-term whole-body vibration were investigated. Vibrational prostatopathy was characterized by more incident and pronounced decrease in prostate size, blurred contours, and appearance of sites with changed density (fibrosis, calcification, cysts) in central and peripheral zones of the gland. Vibrogenic prostate remodeling is determined by marked reduction of microvessel and prostatic glands, particularly in the central (periurethral) part, smooth muscle cell hyperplasia and hypertrophy, and marked fibrosis of the stroma in the absence of inflammatory cellular infiltration. Morphological data describing reduction of microvessels in the prostate caused by whole-body vibration correlate with Doppler scanning data indicating reduced perfusion of the organ.

**Key Words:** whole-body vibration; prostate; Doppler ultrasonic scanning; pathomorphology, ultrastructure

Investigation of local and whole-body vibration effects on human body, organs, and tissues is prompted by significant distribution of this factor and its role in vital functions [8]. Unfavorable effects of vibration consist in not only unpleasant sensations, but also various pathologies, *e.g.* vibration disease [3,7]. These processes are of special interest for specialists exposed to vibration for a long-time: drivers and skimmers. Apart from known symptoms of vibration disease, based on microangiopathy and visceropathies [6,7], chronic prostate diseases and disturbances in male reproductive functions associated with these conditions were recently added [4,5,10]. At the same time, the effects of vibration as a wide-spread occupational hazard factor on the prostate and its hemodynamics are little studied.

The objective of this study was to investigate pathomorphological changes and blood supply in

the prostate gland (PG) during long-term exposure to whole-body vibration.

### MATERIALS AND METHODS

Clinical and functional examination of 31 patients (agricultural engineers with long-term whole-body vibration exposure) with chronic prostatitis was performed. Mean age of the examinees was  $54.2 \pm 6.7$ ; 96.8% of them had length of service in this branch 10-39 years (mean  $27.5 \pm 5.6$ ); the history of chronic prostatitis was  $8.6 \pm 5.3$  years (from 1 to 20 years). Microscopic investigation and immunoassay of the urethra content for sexually transmitted infections were performed in all patients. Patients with verified venereal infection were not included in the study.

Examination of PG biopsy samples was of special interest, because it is the most reliable method for detecting of neoplastic transformations and assessment of structural reactions to adverse exposure [12]. Fine-needle PG biopsy samples were obtained from 23 patients (mean age  $52.1 \pm 5.7$  years, expo-

Research Institute of Regional Pathology and Pathomorphology, Siberian Division of the Russian Academy of Medical Sciences, Novosibirsk; \*Altai State Medical University, Federal Agency for Health Care and Social Development, Barnaul, Russia. **Address for correspondence:** pathol@soramn.ru. E. L. Lushnikova

sure to whole body vibration  $24.8 \pm 6.1$  years) from the central and peripheral areas. Small samples ( $\sim 1 \text{ mm}^3$ ) were separated from obtained biopsy samples (tissue stabs 4-15 mm long and approximately 1 mm wide), fixed in 4% paraformaldehyde, post-fixed in osmium tetroxide, and embedded into epon and araldite for preparation of semithin and ultrathin sections. Other fragments were fixed in 10% neutral formalin to obtain paraffin sections.

Paraffin sections were stained with hematoxylin and eosin, van Gieson's stain, passed through PAS-reaction. Semithin sections were stained with azure II. The paraffin and semithin sections were examined under an all-purpose light Leica DM 4000B microscope. Micrographs were obtained using a Leica DFC 320 digital camera and Leica QWin V3 software. Ultrathin sections contrasted with uranyl acetate and lead citrate were analyzed under a JEM 1010 electron microscope at accelerating voltage 40 kV.

Functional examination included ultrasonic PG examination (Hitachi-515) and Color Doppler PG Imaging. During ultrasonic examination, we evaluated the proportions, volume, symmetry, and contours of PG, the state of the capsule and seminal vesicle, and the presence of additional structures. Doppler ultrasound examination was performed according to routine protocol with consecutive transabdominal and transrectal scanning [2,9]. Standard ultrasonic convex sensors with frequency 3.5 MHz for transabdominal and 47.0 MHz for transrectal scanning were used. PG shape, proportions, echogenicity, and echostructure were assessed in B-mode using well-established criteria [9].

For evaluation of normal PG proportions and functional characteristics, 11 volunteers were examined (control group). They all were considered to be healthy on the basis of integrated urological examination including physical examination, digital rectal investigation, transabdominal and transrectal ultrasonic PG scanning.

Quantitative data were processed with adequate statistic methods using Microsoft Excel 2000 and Statistica 6.0 (StatSoft Inc.).

## RESULTS

Patients exposed to whole-body vibration for many years reported difficult (45.2% participants) and frequent (29% patients) urination as subjective signs of PG pathology. Vibration prostatopathy was characterized by predominance of infravesical obstruction, while signs of irritation and urethra discharges were rare.

Transrectal ultrasonic examination revealed various pathological changes in all patients exposed

to whole-body vibration: the size of PG was normal in 18 patients (58.1%) and reduced in 10 subjects (32.3%), insignificant increase in PG size was noted in 3 patients (9.7%). In 14 participants (45.2%), PG had clear-cut and smooth contours, while in 17 patients (54.8%) PG contours were blurred and interrupted. Echostructure of PG was changed (heterogeneous) in all patients (100%): areas with high echogenicity (fibrosis, calcified foci, infiltrations) and low echogenicity were seen. Hyper- and hypoechogenic inclusions 2-4 mm in size were found in PG. It should be noted that changes were diffuse with involvement of central and peripheral PG areas, while in patients with chronic prostatitis without exposure to vibration these changes are usually localized in peripheral areas of the organ [4,10].

The pattern and intensity of pathomorphological changes in the central and peripheral areas were compared by light microscopy. Mucous (internal) prostatic glands with terminal parts lined with single-layer (rare with double-row) cubical or columnar epithelium are normally located in the central (periurethral) area of PG. Branched terminal parts of principal (external) prostatic glands are located in the peripheral area and mainly constitute its mass. Intermediate area located between the central and peripheral areas consists of submucosal (intermediate) glands. The excretory ducts of mucosal glands are open into the urethra, while the excretory ducts of submucosal and principal glands are open on the borders of seminal colliculus. PG stroma is presented by a large number of vessels and nerve fibers. Each PG zone includes smooth muscle cells, myofibroblasts, fibroblasts, and collagen fibers [14]. The terminal parts of the glands and excretory ducts are surrounded by wide fibromuscular bands (with big amount of elastic fibers) connected with organ capsule. Their contractions promote discharge of the prostatic gland secretion into the urethra.

Examination of biopsy samples obtained from the peripheral areas of PG from patients exposed to whole body vibration revealed decreased number and size of principal glands. The lumens of these glands on sections had folded relief and contained fragments of desquamated epithelial cells, small vesicular formations (probably apical parts of epithelial cells with secretory granules), prostatic concretions (concretions, stones) of various shape and size (Fig. 1, *a*). In some glands, prostatic concretions were large and had primarily stratified structure; they formed conglomerations and completely occluded the gland lumen. Structural reorganization of the terminal parts of principal glands varied from focal destruction and atrophy to squamous cell metaplasia (Fig. 1, *b*). Adenomes with mar-



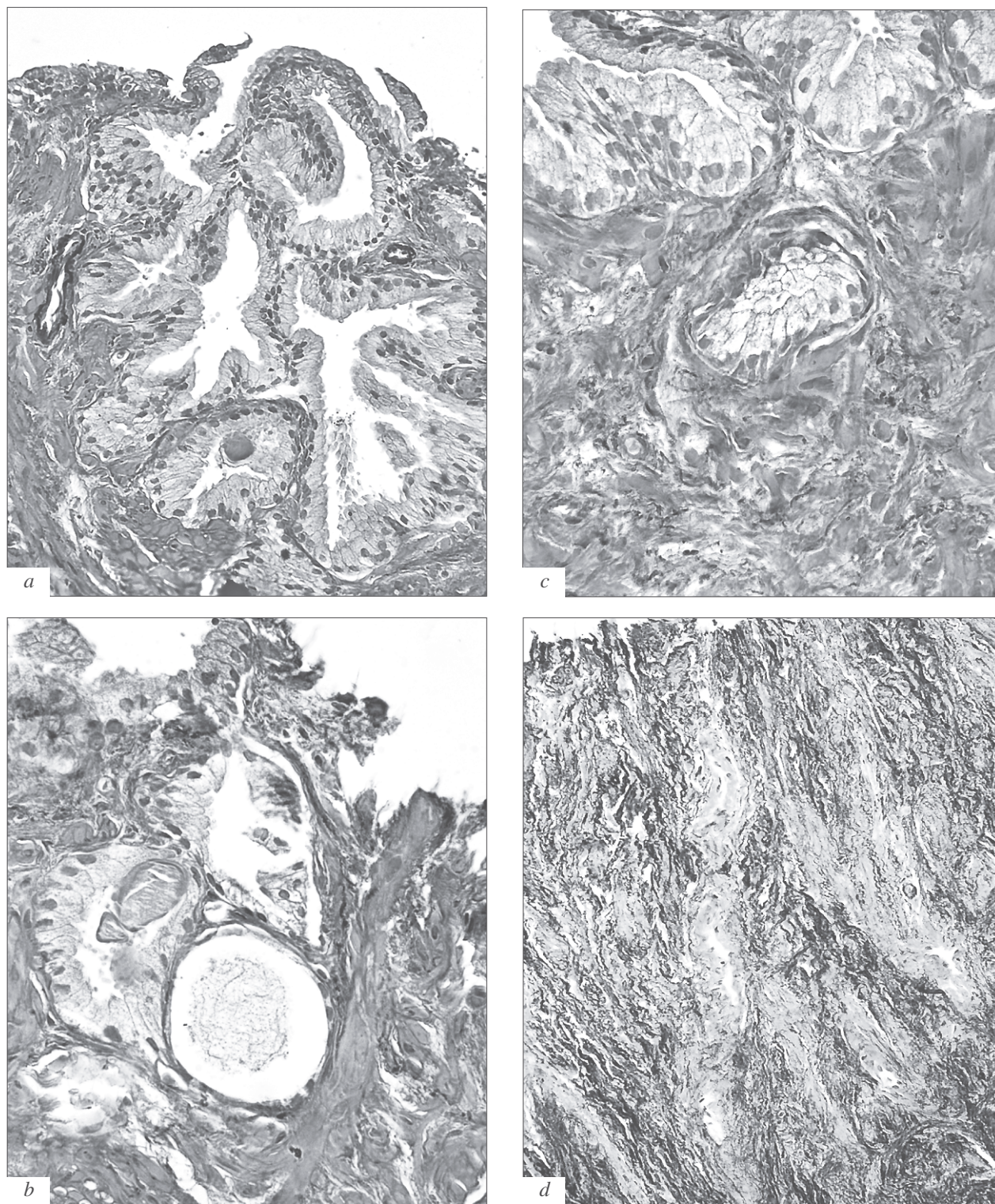


**Fig. 1.** Structural changes in PG after exposure to whole body vibration; van Gieson staining. *a*) desquamated epithelial cells, vesicular structures, and a concretum in lumens of principal prostatic glands,  $\times 250$ ; *b*) diversity of structural changes in epithelial lining (from focal destruction and atrophy to squamous-cell metaplasia) in terminal parts of principal prostatic glands,  $\times 400$ ; *c*) pronounced fibrosis and hyperelastosis of the connective tissue-muscular stroma of the gland,  $\times 400$ ; *d*) atrophy of mucous (periurethral) glands, marked hyperelastosis and collagenosis of the stroma,  $\times 400$ .



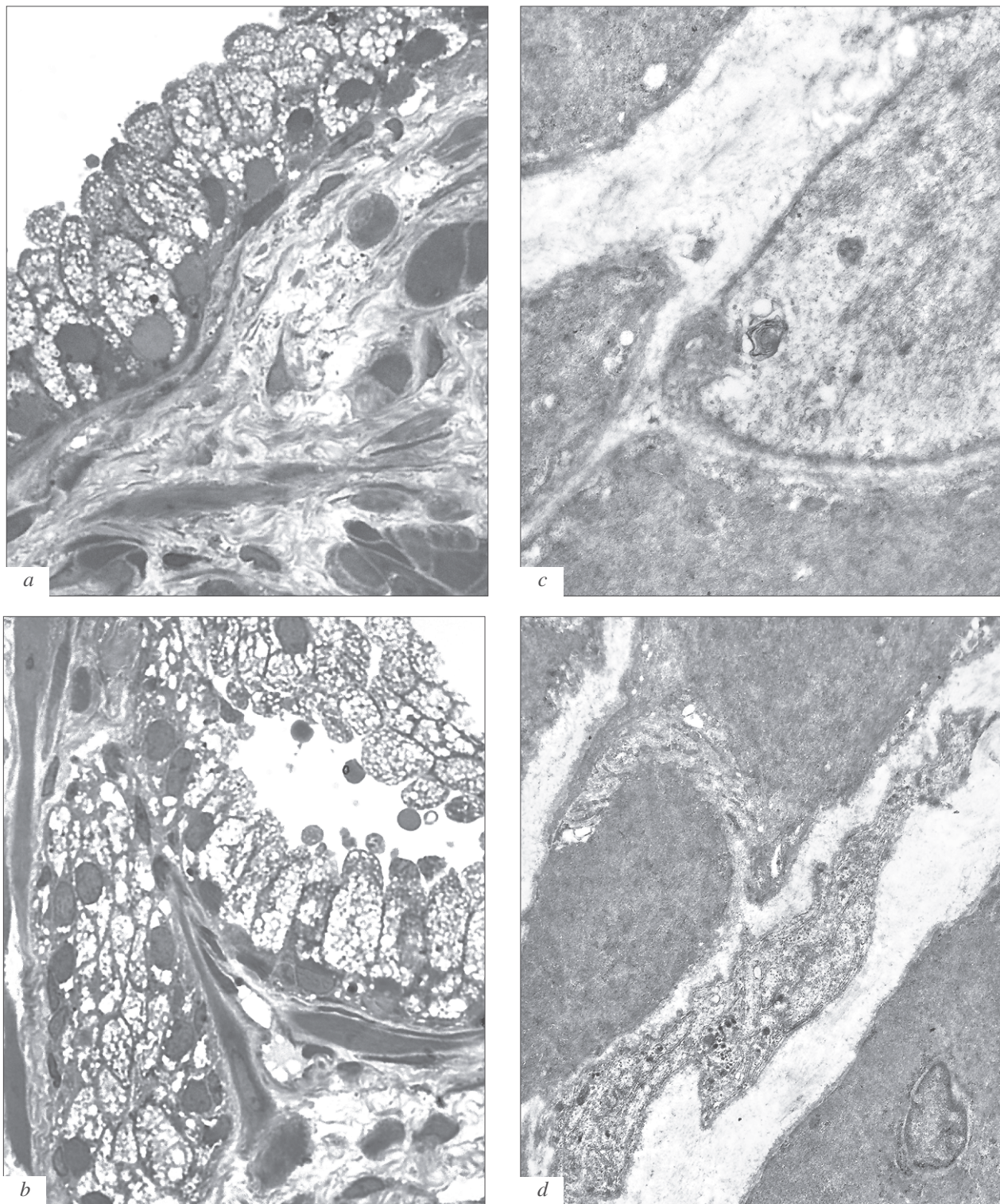


**Fig. 2.** Morphological changes in epithelial and smooth muscle cells of PG caused by exposure to whole-body vibration. *a*) prevalence of the principal secretory epithelial cells in epithelial lining, collagenosis of adjacent stroma. Semithin section, azur II staining,  $\times 1000$ ; *b*) separation of apical fragments of the principal secretory epithelial cells into gland lumen. Semithin section, azur II staining,  $\times 1000$ ; *c*) heterogeneity of smooth muscle cells, formation of myelin-like structures in the sarcoplasm,  $\times 10,000$ ; *d*) fragments of smooth muscle cells and activated fibroblasts,  $\times 6000$ .

kedly flattened epithelial lining and partial desquamation often contained huge concretions.

In most cases, terminal parts of principal gland were lined with double-row columnar epithelium (Fig. 2, *a*). Epithelial lining looked like a multilayer only on tangential sections of folds protruding into the gland lumen and formed by epithelium and adjacent connective tissue. The main cell population of epithelial lining was presented by principal (secretory) cells with nucleus shifted to the basement membrane and great amount of secretory granules in the central and apical cytoplasm. Rare basal cells contained hyperchromatic nuclei surrounded by thin cytoplasmic rim. It should be noted that secretory activity was preserved in the majority of principal cells. Separation of apical parts of the principal epithelial cells (kind of clasmotosis) with secretory granules was often observed (Fig. 2, *b*). These numerous lumps in terminal parts of principal prostatic gland are probably a structural basis for the formation of prostatic concretions and calcificates. Thickening of the basement membrane in terminal parts of glands accompanied by marked fibrosis of the subepithelial connective tissue was also seen (Fig. 2, *b*).

The stroma of the peripheral PG area generally consisted of thickened bundles of hypertrophic smooth muscle cells surrounded by numerous collagen and elastic fibers (Fig. 1, *c*). Extensive hyperelastosis was most pronounced near terminal parts of the glands. Irregularly distributed elastic fibers formed polymorphic structures. The number of capillaries in the subendothelial stroma was decreased and most of them were aneurysmally changed. In the majority of blood vessels, structural and functional heterogeneity of endotheliocytes (hypertrophy, dystrophy, necrobiosis) was observed. Inflammatory

infiltration in glands and the connective tissue-muscular stroma was absent.

Smooth muscle cells forming the stroma of peripheral PG area were characterized by marked dystrophic changes. Light microscopy revealed empty zones around the nucleus; electron microscopy showed marked heterogeneity of smooth muscle cells: cells with electron-dense and moderately dense cytoplasm were distinguished (Fig. 2, *c*). Cells with moderately dense cytoplasm virtually always contained myelin-like structures and few profiles of vesicles and cisterns of the endoplasmic reticulum. Ultrastructure of smooth muscle cells was monomorphic due to prevalence of actin myofilaments (Fig. 2, *d*). Activated fibroblasts were often seen between smooth muscle cells.

In biopsy samples from the periurethral area of PG from patients exposed to whole-body vibration, prostatic glands were virtually absent. The tissue fragments were presented by fibrous stroma with solitary blood vessels (Fig. 1, *d*). Similarly to the peripheral area, numerous thickened smooth muscle bundles surrounded by thickened collagen fibers were seen. The zone was characterized by pronounced hyperelastosis, thickened elastic fibers were comparable in size with collagen fiber bundles. Similarly to the central area, inflammatory cellular infiltration was also absent.

Assessment of PG vascularization and hemodynamics revealed marked changes. Exposure to the occupational hazard factor decreased the diameter of visualized vessels by 1.9 times in the central part and by 2.1 times in the peripheral area compared to normal values (Table 1). The density of the vascular plexus was reduced by 4.1 times in the central and peripheral parts. Peak linear blood flow velocity in the central and peripheral PG areas

**TABLE 1.** PG vascularization and hemodynamics parameters in patients, exposed to long-term whole-body vibration ( $M \pm m$ )

Parameter	Healthy men ( $n=11$ )		Patients exposed to whole body vibration ( $n=31$ )	
	CZ	PZ	CZ	PZ
Peak linear speed ( $V_p$ ), cm/sec	12.91 $\pm$ 0.74	11.86 $\pm$ 0.45	5.86 $\pm$ 0.48*	5.40 $\pm$ 0.41*
Linear diastolic speed ( $V_d$ ), cm/sec	4.97 $\pm$ 0.31	4.210 $\pm$ 0.025	2.25 $\pm$ 0.40*	1.91 $\pm$ 0.25*
Mean linear speed ( $V_m$ ), cm/sec	8.08 $\pm$ 0.43	7.37 $\pm$ 0.26	4.01 $\pm$ 0.41*	3.35 $\pm$ 0.38*
Pulse index (PI), arb. units	0.960 $\pm$ 0.014	1.030 $\pm$ 0.043	1.61 $\pm$ 0.04*	1.23 $\pm$ 0.01*
Resistance index (RI), arb. units	0.600 $\pm$ 0.014	0.640 $\pm$ 0.019	0.800 $\pm$ 0.024*	0.81 $\pm$ 0.024*
Vessel diameter ( $D_m$ ), cm	0.060 $\pm$ 0.004	0.060 $\pm$ 0.004	0.031 $\pm$ 0.003*	0.029 $\pm$ 0.002*
Flow volume (FV), liter/min	0.029 $\pm$ 0.002	0.026 $\pm$ 0.002	0.009 $\pm$ 0.001*	0.006 $\pm$ 0.001*
Vascular plexus density (VPD), vessel/cm <sup>3</sup>	2.250 $\pm$ 0.195	1.20 $\pm$ 0.35	0.55 $\pm$ 0.34*	0.29 $\pm$ 0.19*

**Notes:** CZ: central zone, PZ: peripheral zone. \* $p < 0.001$  compared to healthy men.



decreased by 2.2 times, the mean diastolic linear blood flow velocity also decreased in both areas. The mean linear blood flow velocity in the central area decreased 2-fold and in the peripheral area by 2.2 times. These changes determined decreased volume flow rate in PG, which attested to impaired hemodynamics. The mean value of pulse index in the central and peripheral PG areas increased by 1.7 and 1.2 times, respectively; the resistance index increased by 1.3 times in both areas.

The data of Doppler ultrasonic study and pathomorphological examination in patients exposed to whole-body vibration for a long time attested to marked impairment of blood supply to the organ primary due to reduction of blood vessels. Microvascular disturbances or systemic microangiopathies belong to the most persistent and manifest symptoms of vibration disease and play the key role in the pathogenesis of this disease: they disturb transcapillary exchange and cause plastic (trophic) deficit in tissues [7]. At the same time, vibration is an extreme physical factor which simultaneously mediates the development of the general adaptation syndrome and affects various structural and functional elements of the organism (from molecules to supramolecular structures) altering their physicochemical properties. These processes lead to the development of multiorgan dystrophic-atrophic failure and involutive remodeling of tissues and organs with marked diffuse fibrosis of the connective tissue stroma.

Thus, long-term exposure to whole-body vibration leads to marked dystrophic-atrophic changes and reduction of prostatic glands, especially in the central (periurethral) PG zone. These changes correlate with reduction of microvessels and are accompanied by hyperplasia and hypertrophy of smooth muscle cell forming thickened muscle bundles in the organ stroma. Diffuse fibrosis (collagenosis and

elastosis), more pronounced in the central zone, is a crucial point of vibrogenic PG remodeling. It should be noted, that the observed pathomorphological changes in PG caused by exposure to whole-body vibration differ from those during chronic prostatitis [4,10,11,13], in particular by the absence of inflammatory cell infiltration. This allows us to define the whole complex of revealed changes as vibration prostatopathy [1] similarly to other organopathies described in vibration syndrome [6,7].

## REFERENCES

1. V.A. Anan'ev, A. I. Neymark, and N. V. Nazarenko, *Sibirsk. Med. Zh.*, **76**, No. 1, 99-101 (2008).
2. V. P. Kulikov, *Color Duplex Scanning in Vascular Disease Diagnosis* [in Russian], Novosibirsk (1997).
3. M. M. Mel'nikova, *Medicina Truda i Prom. Ekologia*, No. 5, 36-41 (1995).
4. V. A. Molochkov and I. I. Il'in, *Chronic Urethrogenic Prostatitis* [in Russian], Moscow (2004).
5. A. I. Neymark, *Diseases of Male Reproductive Organs. Therapy and Prophylactics* [in Russian], Barnaul (1992).
6. G. I. Nepomnyashchikh, N. A. Abdullaev, S. V. Aidagulova, et al., *Bull. Exp. Biol. Med.*, **142**, No. 11, 585-588 (2006).
7. T. M. Sukharevskaya, A. V. Efremov, G.I. Nepomnyashchikh, et al. *Microangio- and Visceropathies in Vibration Disease* [in Russian], Novosibirsk (2000).
8. K. V. Frolov, *Vibration Biomechanics* [in Russian] Moscow (1989).
9. A. F.Tsyb, G. N. Grishin, and G. V. Nestaiko, *Ultrasonic Tomography and Target Biopsy in Small Pelvis Tumor Diagnostics* [in Russian], Moscow (1994).
10. V. V. Shchetinin and E.A. Zotov, *Prostatitis* [in Russian], Moscow (2003).
11. M. Collins McNaughton, R. MacDonald, and T. J. Wilt, *Ann. Intern. Med.*, **133**, No 5, 367-381 (2000).
12. K. C. Potter, H. Evans, and U. Patel, *Imaging*, **17**, 122-129 (2005).
13. A. J. Schaeffer, *N. Engl. J. Med.*, **355**, No. 16, 1690-1698 (2006).
14. Y. Zhang, S. Nojima, and H. Nakayama, et al., *Oncol. Rep.*, **10**, No. 1, 207-211 (2003).